Power rating and energy yield of hybrid CPV/flat-plate PV modules

Cite as: AIP Conference Proceedings **2550**, 060003 (2022); https://doi.org/10.1063/5.0099267
Published Online: 02 September 2022

Juan F. Martínez, Marc Steiner, Maike Wiesenfarth, et al.

Power Rating and Energy Yield of Hybrid CPV/Flat-Plate PV Modules

Juan F. Martínez[a)], Marc Steiner, Maike Wiesenfarth, Gerald Siefer and Frank Dimroth[1]

Fraunhofer Institute for Solar Energy Systems ISE, Heidenhofstr. 2, 79110 Freiburg, Germany

[a)]Corresponding author: juan.francisco.martinez.sanchez@ise.fraunhofer.de

Abstract. This article summarizes the IEC compliant power rating procedure applied to a hybrid CPV/PV module of the EyeCon technology which uses III-V four-junction CPV cells in combination with bifacial c-Si PV cells. The combined power output of both solar cell types at standard test conditions reached 342 W/m^2, which corresponds to a world record efficiency of 34.2% for the conversion of the reference AM1.5g spectrum. For the first time, we present the annual energy yield of the 4J EyeCon module for the six reference climate zones defined in the energy rating standard IEC 61853-4. When comparing the hybrid yield with the highest electrical generation between conventional CPV and flat-plate PV modules, we found that hybrid CPV/PV technology delivers a maximum energy surplus of 20% in temperate continental climate.

INTRODUCTION

Hybrid concentrator/flat-plate photovoltaic (CPV/PV) technology [1–4] integrates concentrator multi-junction solar cells and flat-plate PV cells within the same module, as shown in Figure 1a. In this manner, the direct normal irradiance (DNI) is concentrated onto the CPV cells by the primary optics, whereas the transmitted diffuse irradiance (DIF) is absorbed by the flat-plate solar cells, as shown in Figure 1b. Furthermore, the use of bifacial PV cells also enables the conversion of the reflected back normal irradiance (BNI) into electricity.

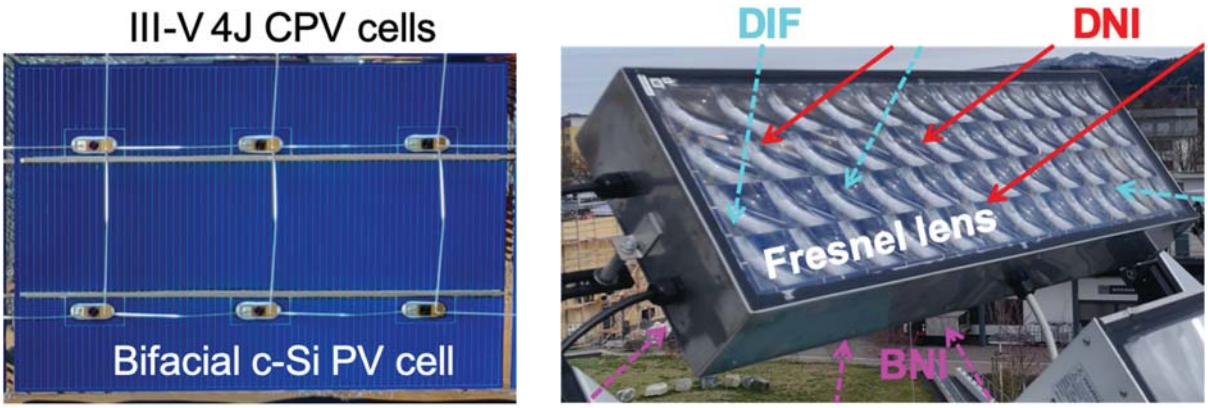

FIGURE 1. Unit cell of a hybrid CPV/PV module showing the (a) architecture of the EyeCon module where underneath the silicone-on-glass Fresnel lenses the III-V multi-junction CPV cells are mounted onto a bifacial c-Si PV cell using a dielectric thermal adhesive and (b) its optical functionality as the direct normal irradiance (DNI) is concentrated onto the CPV cells, whereas the transmitted diffuse (DIF) and reflected back normal irradiances (BNI) are absorbed by the bifacial PV cell.

17th International Conference on Concentrator Photovoltaic Systems (CPV-17)
AIP Conf. Proc. 2550, 060003-1–060003-8; https://doi.org/10.1063/5.0099267
Published by AIP Publishing. 978-0-7354-4392-1/$30.00

In this article, we summarize the power rating procedure developed in [5] and applied to a hybrid CPV/PV module of the EyeCon technology [6, 7]. Such module is equipped with III-V wafer-bonded four-junction (4J) CPV cells, bifacial p-PERC c-Si PV cells and silicon-on-glass Fresnel lenses that yield a geometrical concentration of 321-fold. In addition, this work presents for the first time the evaluation of the annual energy yield of the bifacial 4J EyeCon module under the six reference climate profiles defined in the IEC 61853-4 standard [8] for the energy rating of PV modules. Finally, we also estimated the annual energy yield for conventional CPV and flat-plate PV technologies to compare them with the hybrid CPV/PV yield in order to quantify its advantage in each climate zone.

POWER RATING

The power output of the 4J EyeCon module was rated at standard test conditions (STC) following the procedure described in [5]. The first step consists on the independent acquisition of the light I-V curves (LIV) of the CPV and flat-plate PV arrays as depicted in Figure 2a. Subsequently, the procedure defines the STC for hybrid CPV/PV modules identically as for flat-plate PV modules since both harvest global irradiance. However, it specifies that the CPV solar cells of a hybrid module should be illuminated with the reference AM1.5d spectrum [9], whereas the flat-plate PV cells should be tested with the reference diffuse spectrum, i.e. the difference between the reference AM1.5g and the AM1.5d spectra, at a cell temperature of 25ºC. This is achieved by applying the data filtering criteria defined in the CPV standard IEC 62670-3 [10], while also filtering for global spectral matching ratios [11] between the top and middle isotype cells within ±3% of unity. In this way, the response of the module can be considered as rated under stable and close to AM1.5g conditions. Afterwards, the color-coded flow chart in Figure 2a specifies the usage of the CPV (red) [10], flat-plate PV (blue) [12–15] and bifacial PV (purple) [16] IEC standards, in combination with the necessary modifications (green) developed in [5] to account for the particular features of 4-terminal hybrid CPV/PV modules with dual-axis solar tracking.

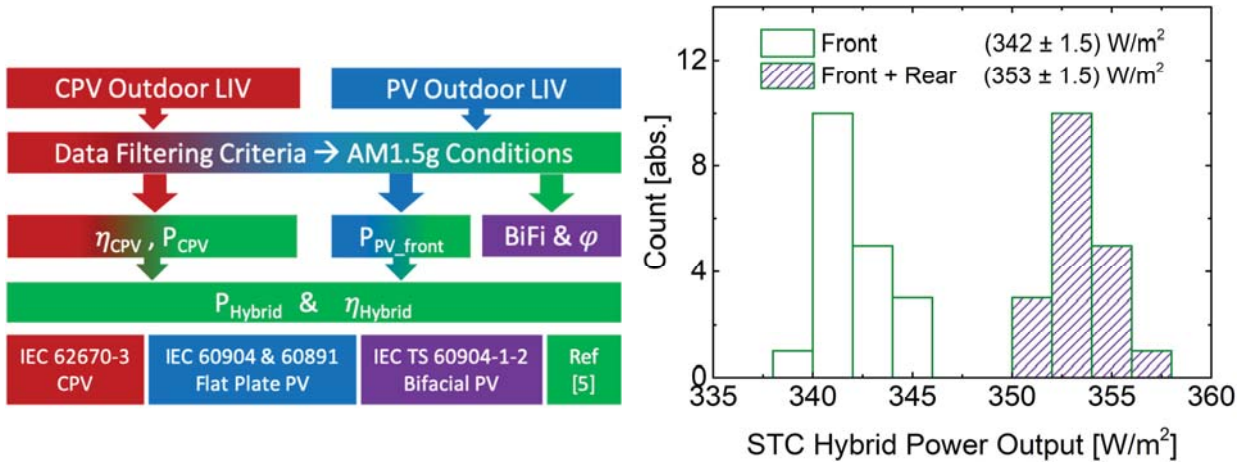

(a) (b)

FIGURE 2. Summary of the power rating (a) procedure for hybrid CPV/PV modules developed in [5] and (b) of the STC results for the 4J EyeCon module under front illumination with the AM1.5g spectrum (hollow bars) and under front plus additional rear side intensity of 100 W/m^2 (hatched bars). The procedure is based on the IEC standards of CPV, flat-plate PV and bifacial PV modules to properly measure the light current-voltage (LIV) curves of the solar cell arrays, determine the filtering criteria to obtain similar to AM1.5g spectral conditions, translate the efficiency (η) and power output (P) of the CPV and flat-plate PV arrays to STC, as well as to determine the bifacial power output gain (BiFi) and the bifaciality factor (φ) of the bifacial PV array.

In this way, the 4J CPV array efficiency (η_{CPV}) and power output (P_{CPV}) were rated at STC as 36.1% and 325 W/m^2, whereas the front power contribution (P_{PV_front}) from the flat-plate solar cells was rated as 16.9 W/m^2. As shown in Figure 2b, this yields a hybrid power output of 342 W/m^2 (hollow bars), which corresponds to a world record efficiency of 34.2% for the conversion of the AM1.5g spectrum [17]. In addition, the bifacial cells have a bifacial power gain (BiFi) of 10.9 W/m^2 for every 100 W/m^2 of rear side irradiance due to the 65% bifaciality factor (φ) of the module. Therefore, the 4J EyeCon module is able to generate over 350 W/m^2 under bifacial illumination (hatched

bars), which is the highest power output density of any PV technology. All the details regarding the power rating procedure for hybrid CPV/PV modules can be found in [5].

ANNUAL ENERGY YIELD

Two empirical power output models [18, 19] were used to calculate the annual energy yield of six photovoltaic technologies. As shown in Table 1, these comprehend hybrid CPV/PV, conventional CPV and monofacial as well as bifacial flat-plate PV modules with single-axis tracking and in fixed-tilt orientation. It is important to note that the reported efficiency of all modules is rated under the global spectrum at STC, except for the conventional CPV module which is rated under the direct spectrum at concentrator standard test conditions (CSTC).

TABLE 1. Summary of the module characteristics of the six different investigated PV technologies.

Technology	Module Type	Solar Cells	Tracking	η_{STC}	Bifaciality Factor	Ground Clearance
Hybrid CPV/PV	EyeCon	III-V 4J + Bifacial c-Si	Dual-axis	34.2 %	65%	4 m
CPV	FLATCON®	III-V 4J	Dual-axis	36.7%*	0%	4 m
Bifi PV 1-axis	Flat-plate	Bifacial c-Si	Single-axis	20%	90%	1 m
Mono PV 1-axis	Flat-plate	Monofacial c-Si	Single-Axis	20%	0%	1 m
Bifi PV fixed-tilt	Flat-plate	Bifacial c-Si	Fixed-tilt	20%	90%	0 m
Mono PV fixed-tilt	Flat-plate	Monofacial c-Si	Fixed-tilt	20%	0%	0 m

*Rated at concentrator standard test conditions (CSTC), i.e. 25ºC, DNI of 1000 W/m^2, AM1.5d spectral distribution.

The annual energy yield of 4J CPV cells is calculated using the empirical power output model validated in Freiburg, Germany and in Sevilla, Spain by Peharz [19]. This multi-linear regression model calculates the CPV power output as the product of the I-V characteristics, i.e. $P_{CPV} = I_{SC} \cdot FF \cdot V_{OC}$. Furthermore, it models the I_{SC} as a function of DNI, T_{amb} and spectral parameter $Z_{1\text{-}2}$ [20–22] to accurately consider current mismatch due to atmospheric scattering of sunlight, as well as chromatic aberration and light spillage due to the temperature dependence of the Fresnel lenses. Moreover, we refined the I_{SC} modeling by including the effect of sunlight absorption due to precipitable water, which is quantified by the spectral parameter $Z_{1\text{-}3}$ [20–22]. Similarly, the FF is modeled as a function of DNI, T_{amb} and $Z_{1\text{-}2}$ in order to account for ohmic and thermal effects, as well as for sub-cell current mismatch. In the case of the V_{OC}, it is modeled only as a function of DNI and T_{amb} since the spectral influence is negligible.

The annual energy yield of bifacial flat-plate PV cells is calculated using the empirical power output model validated for 18 different c-Si modules by Huld et al [18]. This multi-linear regression model calculates the flat-plate PV power output as a function of the normalized effective irradiance, $G = SMM \cdot (G_{front} + \varphi \cdot G_{rear}) / G_{ref}$, and the temperature gradient, $T = T_{cell} - T_{ref}$, between the solar cell and a reference value, i.e. $P_{PV} = f(G, T)$. Furthermore, G considers the effect of spectral variation through the spectral mismatch factor (SMM) [14] as explained by Huld et al in [23], and the absorption of rear side irradiance through the bifaciality factor (φ) as stipulated in [16].

A detailed explanation regarding the usage of the CPV and flat-plate PV power output models, along with the equations and regression coefficients for the 4J EyeCon, the 4J FLATCON® and the flat-plate PV modules can be found in [24]. In addition, hybrid and CPV modules are always assumed normal to the sun, whereas the inclination of flat-plate PV modules was optimized for each climate profile. As shown in Table 2, the optimum tilt angle increases more rapidly with latitude for bifacial flat-plate modules, because a larger inclination boosts the collection of rear side irradiation more than it decreases the absorption on the front side.

For the energy yield calculation, we used the spectral and atmospheric hourly data given in the IEC 61853-4 [8] standard for the six reference climate zones. In increasing order of diffuse fraction these are: subtropical arid, high elevation, temperate continental, subtropical coastal, tropical humid and temperate coastal. A summary of the spectral and meteorological conditions for each climate profile is given in Table 2. The direct, diffuse, global and rear side irradiations are presented as annual sums calculated with the hourly DNI, extraterrestrial, global and diffuse horizontal irradiance (GHI and DHI), the solar position, the module orientation, the sky and ground view factor [25] and the Perez anisotropic sky model [26]. Direct and diffuse irradiance losses due to the angle of incidence are also considered for flat-plate PV modules [27]. The spectral irradiation parameters, i.e. $Z_{1\text{-}2}$, $Z_{1\text{-}3}$ and SMM, which characterize the

response of the CPV and flat-plate PV cells are presented as mean values with their respective standard deviations after calculation with Equations 1-3

$$J_{ph} = \int_0^{\infty} SR(\lambda) \cdot E(\lambda)\, d\lambda \tag{1}$$

$$Z_{i-j} = 2 \cdot \frac{J_{ph\_i}}{J_{ref\_i}} \Big/ \left(\frac{J_{ph\_i}}{J_{ref\_i}} + \frac{J_{ph\_j}}{J_{ref\_j}} \right) - 1 \tag{2}$$

$$SMM = \frac{J_{ph\_Si}}{GNI} \Big/ \frac{J_{ref\_Si}}{1000\ W/m^2} \tag{3}$$

where J_{ph} and J_{ref} are the generated photo-currents of the i^{th} and j^{th} sub-cells of a 3J component cell and of the c-Si reference cell under the spectral irradiance data, E(λ), given in the IEC 61853-4 standard and under the reference spectrum, whereas SR(λ) corresponds to their spectral response. It is important to note that the hourly spectral irradiance data of each climate zone is given in 29 Kato bands ranging from 307 to 4606 nm [28]. Furthermore, it corresponds to the global spectrum on a surface tilted 20º towards the equator. Therefore, we assumed that all the irradiance components, i.e. direct, diffuse and rear side, that we transposed to the different fixed-tilt and tracked planes have this spectral distribution. In reality, not even the reference AM1.5 global, direct and diffuse spectra have the same spectral distribution. Therefore, the uncertainty associated with this assumption remains as a task to be investigated in future work.

TABLE 2. Summary of the atmospheric, irradiation and spectral conditions of the six climate profiles defined in the IEC 61853-4 standard transposed to a dual-axis tracked plane, as well as to optimally tilted planes with and without single-axis tracking.

Climate Profile *(Location/Lat)*	**Subtropical Arid** *(Phoenix/34º)*	**High Elevation** *(Tibet/34º)*	**Temperate Continental** *(Alberta/57º)*	**Subtropical Coastal** *(Japan/33º)*	**Tropical Humid** *(Gabon/1º)*	**Temperate Coastal** *(Glasgow/56º)*
Mean Atmospheric Parameters						
T_{amb} [ºC]	19.5 ± 9.6	-5.4 ± 9.9	2.5 ± 12.8	16.0 ± 8.9	24.1 ± 2.2	8.4 ± 4.8
V_{wind} [m/s]	1.8 ± 0.9	2.8 ± 1.7	2.1 ± 1.0	2.6 ± 1.9	1.0 ± 0.4	3.2 ± 1.8
Albedo [-]	0.16	0.25	0.13	0.12	0.11	0.18
Optimum Tilt Angle for Fixed-Tilt and Single-Axis Tracked Modules						
Monofacial	32º	36º	45º	28º	1º	38º
Bifacial	37º	42º	49º	35º	1º	49º
Annual Dual-Axis Tracked Plane Irradiation [kWh/m²]						
Direct	2428.8	2078.5	1191.5	998.7	1028.4	681.2
Diffuse	769.7	866	602.4	797.4	1033.7	629.7
Rear	343.2	446.8	202.7	226.1	247.2	220.9
Annual Single-Axis Tracked Plane Irradiation [kWh/m²]						
Global	3046.9	2791.4	1679.8	1723	1979.3	1231.4
Rear	268.9	355.4	174.9	190.2	174.5	195.7
Annual Fixed-Tilt Plane Irradiation [kWh/m²]						
Global	2294.8	2160.8	1331.4	1436.8	1668.8	988.2
Rear	120.4	168.6	103.4	70.5	2.1	92
Mean Spectral Irradiation Parameters [-]						
DHI/GHI	0.28	0.36	0.45	0.54	0.56	0.63
$Z_{1\text{-}2}$	0.026 ± 0.057	0.017 ± 0.056	0.011 ± 0.060	0.034 ± 0.059	0.060 ± 0.027	0.017 ± 0.060
$Z_{1\text{-}3}$	0.047 ± 0.084	-0.026 ± 0.091	0.044 ± 0.900	0.095 ± 0.127	0.173 ± 0.037	0.075 ± 0.090
SMM	1.011 ± 0.029	0.995 ± 0.039	1.041 ± 0.043	1.036 ± 0.027	1.032 ± 0.026	1.046 ± 0.035

For example, subtropical arid and high elevation climates are attractive for hybrid and CPV technology because they are typically characterized by high direct normal irradiation beyond 2000 kWh/m^2, and mean ambient temperature around 20 and -5ºC, respectively. Nevertheless, in both climates the sum of diffuse and rear side irradiation represents at least an additional 1100 kWh/m^2, thus, this highlights the importance of capturing the global resource.

On the other hand, temperate continental, subtropical coastal and tropical humid climates typically have global irradiations on the fixed-tilt plane in the range of 1500 kWh/m^2, whereas their usual ambient temperatures vary from 2.5 to 16 to 24ºC, respectively. Therefore, these climate conditions are more attractive for flat-plate PV technologies, particularly when single-axis tracking can increase their front and rear irradiation collection by approximately 300 and 120 kWh/m^2. Nevertheless, the amount of available rear side irradiation also depends on the ground clearance and the ground albedo. Thus, the clearances for each technology are given in Table 1 and the broadband yearly-average albedo values which were calculated from satellite data [29] are given in Table 2. The latter were found to vary around 0.14, except in high elevation climate where the average is 0.25 due to the frequent presence of snow.

In temperate coastal climate, it is more common to have global irradiation in the plane of the array below 1000 kWh/m^2, ambient temperatures in the range of 8ºC and higher wind speeds beyond 3 m/s. Hence, this climate is also better suited for flat-plate PV modules.

Regarding the spectral irradiance, a mean $Z_{1\text{-}2} > 0$ for every climate indicates stronger scattering of sunlight between 600 and 900 nm than below 600 nm relative to the reference AM1.5d spectrum. For a 4J solar cell, this means that the I_{SC}/DNI of the sub-cell with the largest band gap is larger than under the AM1.5d spectrum. Furthermore, a mean $Z_{1\text{-}3} < 0$ only occurs in high elevation climate due to the lower absorption of sunlight by the water vapor. This indicates that there are more photons beyond 900 nm than below 600 nm relative to the reference AM1.5d spectrum. For a 4J solar cell, this means that the I_{SC}/DNI of the sub-cells which absorb light beyond 900 nm is larger than under the AM1.5d spectrum. For a single-junction c-Si solar cell, a SMM > 1 means that the I_{SC}/GNI (global normal irradiance) is larger than under the reference AM1.5g spectrum. Again, this is true for every climate except at high altitudes where the irradiance surplus due to the lower water content is beyond the absorption range of Si, thus, it does not contribute to photo-current.

The annual energy yield results for every investigated PV technology in every reference climate are presented in Figure 3a. The hybrid CPV/PV yield (black bars) is always highest reaching up to 886 kWh/m^2 in subtropical arid regions, however it decreases down to 340 kWh/m^2 in temperate coastal climate as the annual DNI decreases and the diffuse fraction increases. This behavior is also observed for conventional CPV technology (red bars) which is the runner up until the diffuse fraction goes above 50%. This occurs in subtropical coastal, tropical humid and temperate coastal climate where bifacial flat-plate PV modules with single-axis tracking (green bars) become the closest competitor for hybrid CPV/PV technology. The reason is that single-axis tracking increases in average the yield of fixed-tilt monofacial PV modules (pink bars) by 25%, whereas bifaciality gives them an additional 10% energy boost. Bifacial fixed-tilt (light blue) and monofacial single-axis tracked (blue) PV modules are the intermediate yield flat-plate technologies which result in a higher levelized cost of electricity with respect to bifacial single-axis tracked PV modules [30]. Therefore, the latter substitutes the incumbent monofacial fixed-tilt PV modules as the current technology to beat.

Moreover, we calculated the energy yields of hybrid CPV/PV, conventional CPV and flat-plate PV technologies neglecting the effect of spectral variation ($Z_{1\text{-}2} = Z_{1\text{-}3} = 0$ and SMM = 1) and found mean deviations of +4.8 ± 2.3%, +4.1 ± 2.5% and -0.9 ± 0.1%, respectively (the ± value is the standard deviation over the six climate zones). This underscores the importance of considering the effect of spectral variation in the energy yield calculations. Particularly for multi-junction solar cell technology which is highly susceptible to current mismatch.

The energy yield ratios between hybrid CPV/PV and the other five PV technologies investigated are presented in Figure 3b. The ratio denotes the energy surplus that a hybrid CPV/PV module is able to generate in every climate. This ratio can be understood as the tolerable extra cost before the technologies break even. For example, relative to conventional CPV (red bars), a hybrid module generates 8.5% more energy in high DNI locations with subtropical arid climate. This increases up to 48% in temperate coastal regions where the diffuse fraction is the highest. The opposite trend is found relative to flat-plate PV technologies, with the exception that the lowest energy gains occur in tropical humid climate. This is due to the high scattering and absorption of sunlight beyond 600 nm which limits the current output of the 4J solar cells by the middle sub-cells. Therefore, a hybrid module can generate between 33 and

93% more energy than monofacial fixed-tilt PV technology (pink bars), and between 4 and 35% more than a bifacial single-axis tracked PV module (green bars).

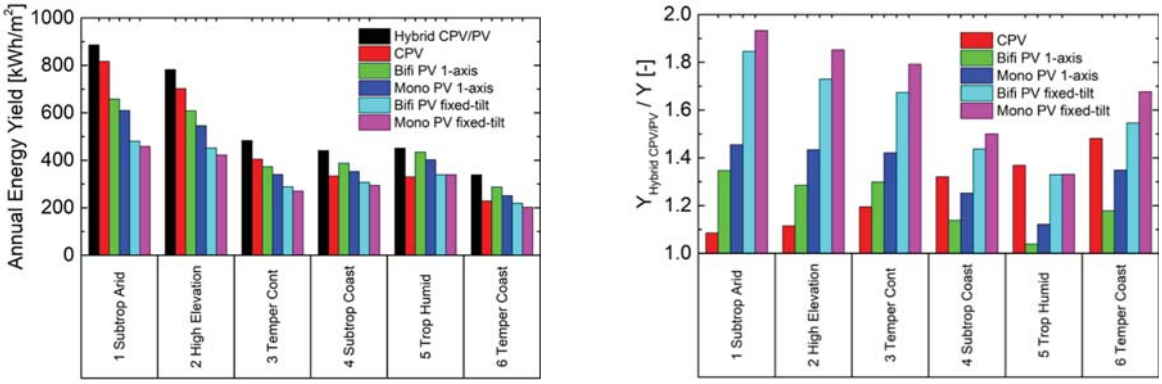

FIGURE 3. Calculated (a) annual energy yields for hybrid CPV/PV (black), conventional CPV (red), single-axis tracked bifacial (green) and monofacial (blue) PV, as well as fixed-tilt bifacial (light blue) and monofacial (pink) PV modules for the six different climate profiles defined in the IEC 61853-4 standard. (b) Yield ratios depicting the additional energy that a hybrid CPV/PV module can generate in each climate zone with respect to the PV technologies mentioned above.

To assess the maximum competitiveness of hybrid CPV/PV technology we need to look at the minimum yield ratio for every climate zone in Figure 3b. This corresponds to the ratio relative to conventional CPV (red bars) in subtropical arid, high elevation and temperate continental climate; and with respect to bifacial single-axis tracked PV (green bars) in subtropical coastal, tropical humid and temperate coastal climate. Thus, a maximum energy gain of 20% with respect to its closest competitor is expected under temperate continental climate.

SUMMARY AND CONCLUSION

This article presents a summary of the IEC compliant power rating procedure for hybrid CPV/PV modules and its application to the 4J EyeCon module [5]. The dual-axis tracked module is equipped with independently interconnected III-V wafer-bonded 4J CPV cells and flat-plate bifacial c-Si PV cells, thus it is a 4-terminal device. At STC, its power output was rated as 342 W/m^2, which corresponds to a world record efficiency of 34.2% for the conversion of the AM1.5g spectrum [17]. Given the usage of bifacial solar cells, the module generates an additional 10.9 W/m^2 for every 100 W/m^2 of rear side irradiance it receives. In this manner, the 4J EyeCon module generates over 350 W/m^2, which is the highest power output per unit area of any PV technology [31].

In addition, we calculated the annual energy yield of hybrid CPV/PV, conventional CPV and flat-plate PV technologies for the six climate zones defined in the energy rating standard for PV modules IEC 61853-4 [8]. Hence, we calculated that the 4J EyeCon module generates more energy than any other PV technology in every climate and that it reaches a maximum yield of 886 kWh/m^2 in subtropical arid regions. However, we found that relative to its closest competitor, i.e. conventional CPV and bifacial single-axis tracked PV modules, hybrid CPV/PV technology offers a maximum energy gain of 20% in temperate continental climate.

Although the system cost per m^2 is not considered, this technical analysis of the performance of the most competitive PV technologies shall be useful to orient and quantify the expectations of any potential deployment of hybrid CPV/PV technology in the field. Further investigation regarding scaling of the system, ground coverage ratio effects and the performance of the EyeCon module as a voltage-matched 2-terminal device, remain as future work tasks.

ACKNOWLEDGMENTS

The authors acknowledge the support of the "III-V Photovoltaics and Concentrator Technology" department at Fraunhofer ISE for their support. We thank the company SOITEC for wafer-bonding of the 4J cells. This work has been financially supported in part by the National Council of Science and Technology (CONACYT) and the Mexican Secretary of Energy (SENER) in the form of a Ph.D. scholarship for Juan F. Martínez. This research has received funding from the European Union's Horizon 2020 research and innovation programme under grant agreement No. 857775. The authors are responsible for the contents of this paper.

REFERENCES

1. J. F. Martínez, M. Steiner, M. Wiesenfarth, and F. Dimroth, "4-Terminal CPV module capable of converting global normal irradiance into electricity," in *14th International Conference on Concentrator Photovoltaic Systems (CPV-14): AIP Conference Proceedings*, Puertollano, Spain, 2018, p. 90005.
2. S. Askins *et al., Eds., Performance of Hybrid Micro-Concentrator Module with Integrated Planar Tracking and Diffuse Light Collection*: IEEE Xplore, 2019.
3. N. Yamada and D. Hirai, "Maximization of conversion efficiency based on global normal irradiance using hybrid concentrator photovoltaic architecture," *Prog. Photovolt: Res. Appl.*, vol. 24, no. 6, pp. 846–854, 2016.
4. K.-T. Lee, Y. Yao, J. He, B. Fisher, X. Sheng, M. Lumb, L. Xu, M. A. Anderson, D. A. Scheiman, S. Han, Y. Kang, A. Gumus, R. R. Bahabry, J. W. Lee, U. Paik, N. D. Bronstein, A. P. Alivisatos, M. Meitl, S. Burroughs, M. M. Hussain, J. C. Lee, R. G. Nuzzo, and J. A. Rogers, "Concentrator photovoltaic module architectures with capabilities for capture and conversion of full global solar radiation," (eng), *Proceedings of the National Academy of Sciences of the United States of America*, vol. 113, no. 51, E8210-E8218, 2016.
5. J. F. Martínez, M. Steiner, M. Wiesenfarth, Siefer, Gerald, Glunz, Stefan W., and F. Dimroth, "Power Rating Procedure of Hybrid CPV/PV Bifacial Modules," *Prog. Photovolt: Res. Appl.*, 2021.
6. J. F. Martinez, M. Steiner, M. Wiesenfarth, S. W. Glunz, and F. Dimroth, "Thermal Analysis of Passively Cooled Hybrid CPV Module Using Si Cell as Heat Distributor," *IEEE J. Photovolt.*, vol. 9, no. 1, pp. 1–7, 2018.
7. J. F. Martínez, M. Steiner, M. Wiesenfarth, T. Fellmeth, T. Dörsam, M. Wiese, S. W. Glunz, and F. Dimroth, "Development and outdoor characterization of a hybrid bifacial HCPV module," *Prog. Photovolt: Res. Appl.*, vol. 9, no. 1, p. 836, 2020.
8. IEC, *Photovoltaic (PV) module performance testing and energy rating - Part 4: 61853-4,* 1st ed. Geneva, Switzerland: International Electrotechnical Commission, 2018.
9. IEC, *Photovoltaic devices - Part 3: 60904-3,* 4th ed. Geneva, Switzerland: International Electrotechnical Commission, 2019.
10. IEC, *62670 CONCENTRATOR PHOTOVOLTAIC (CPV) PERFORMANCE TESTING: Part 3: Performance measurements and power rating, 2017*.
11. C. Domínguez, I. Antón, G. Sala, and S. Askins, "Current-matching estimation for multijunction cells within a CPV module by means of component cells," *Prog. Photovolt: Res. Appl.*, vol. 21, no. 7, pp. 1478–1488, 2013.
12. IEC, *Photovoltaic devices: 60891,* 2nd ed. Geneva, Switzerland: International Electrotechnical Commission, 2009.
13. IEC, *Photovoltaic devices - Part 10: 60904-10,* 2nd ed. Geneva, Switzerland: International Electrotechnical Commission, 2009.
14. IEC, *Photovoltaic devices - Part 7: 60904-7,* 3rd ed. Geneva, Switzerland: International Electrotechnical Commission, 2008.
15. IEC, *Photovoltaic devices - Part 5: 60904-5,* 2nd ed. Geneva, Switzerland: International Electrotechnical Commission, 2011.
16. IEC, *Photovoltaic devices - Part 1-2: TS 60904-1-2,* 1st ed. Geneva, Switzerland: International Electrotechnical Commission, 2019.
17. M. Green, E. Dunlop, J. Hohl-Ebinger, M. Yoshita, N. Kopidakis, and X. Hao, "Solar cell efficiency tables (version 57)," *Prog. Photovolt: Res. Appl.*, vol. 29, no. 1, pp. 3–15, 2021.
18. T. Huld, G. Friesen, A. Skoczek, R. P. Kenny, T. Sample, M. Field, and E. D. Dunlop, "A power-rating model for crystalline silicon PV modules," *Sol. Energy Mater. Sol. Cells*, vol. 95, no. 12, pp. 3359–3369, 2011.

19. G. Peharz, “Untersuchung und Modellierung des Energieertrages von hochkonzentrierenden PV Modulen mit spektral sensitiven Hochleistungssolarzellen,” Dissertation, Fachbereich Physik, Konstanz, Universität, Konstanz, Germany, 2011.
20. G. Peharz, G. Siefer, and A. W. Bett, “A simple method for quantifying spectral impacts on multi-junction solar cells,” *Sol. Energy*, vol. 83, no. 9, pp. 1588–1598, 2009.
21. G. Peharz, G. Siefer, K. Araki, and A. W. Bett, “Spectrometric outdoor characterization of CPV modules using isotype monitor cells,” in *Conference Record of the 33rd IEEE Photovoltaic Specialists Conference*, San Diego, CA, USA, 2008, pp. 1–5.
22. M. Meusel, R. Adelhelm, F. Dimroth, A. W. Bett, and W. Warta, “Spectral Mismatch Correction and Spectrometric Characterization of Monolithic III-V Multi-junction Solar Cells,” *Prog. Photovolt: Res. Appl.*, vol. 10, no. 4, pp. 243–255, 2002.
23. T. Huld and A. Amillo, “Estimating PV Module Performance over Large Geographical Regions: The Role of Irradiance, Air Temperature, Wind Speed and Solar Spectrum,” *Energies*, vol. 8, no. 6, pp. 5159–5181, 2015.
24. J. F. Martínez Sánchez, M. Steiner, M. Wiesenfarth, H. Helmers, G. Siefer, S. W. Glunz, and F. Dimroth, “Worldwide Energy Harvesting Potential of Hybrid CPV/PV Technology,” *SSRN Journal*, 2021.
25. X. Sun, M. R. Khan, C. Deline, and M. A. Alam, “Optimization and performance of bifacial solar modules: A global perspective,” *Appl. Energy*, vol. 212, pp. 1601–1610, 2018.
26. R. Perez, P. Ineichen, R. Seals, J. Michalsky, and R. Stewart, “Modeling daylight availability and irradiance components from direct and global irradiance,” *Sol. Energy*, vol. 44, no. 5, pp. 271–289, 1990.
27. N. Martín and J. M. Ruiz, “Annual angular reflection losses in PV modules,” *Prog. Photovolt: Res. Appl.*, vol. 13, no. 1, pp. 75–84, 2005.
28. A. Amillo, T. Huld, P. Vourlioti, R. Müller, and M. Norton, “Application of Satellite-Based Spectrally-Resolved Solar Radiation Data to PV Performance Studies,” *Energies*, vol. 8, no. 5, pp. 3455–3488, 2015.
29. National Aeronautics and Space Administration, *NASA Earth Observations (NEO).* [Online] Available: https://neo.sci.gsfc.nasa.gov/view.php?datasetId=MCD43C3_M_BSA&date=2015-12-01. Accessed on: Dec. 21 2020.
30. C. D. Rodríguez-Gallegos, H. Liu, O. Gandhi, J. P. Singh, V. Krishnamurthy, A. Kumar, J. S. Stein, S. Wang, L. Li, T. Reindl, and I. M. Peters, “Global Techno-Economic Performance of Bifacial and Tracking Photovoltaic Systems,” *Joule*, vol. 4, no. 7, pp. 1514–1541, 2020.
31. J. F. Martínez, M. Steiner, M. Wiesenfarth, S. W. Glunz, F. Dimroth, J. F. Martinez, and G. Siefer, “Hybrid Bifacial CPV Power Output Beyond 350W/m2,” in *47th IEEE PVSEC*, Virtual Meeting, 2020, pp. 2708–2711.